

66  
UNIVERSITI SAINS MALAYSIA



UNIVERSITI SAINS MALAYSIA

Uniformity, sensitivity, linearity and hot region  
image analysis by employing unconventional  
filter technique (Cu 0.125mm and Al 0.2mm)  
with Tc-99m in SPECT imaging

Dissertation submitted in partial fulfillment for the  
award of the Bachelor's Degree of Health Sciences  
Medical Radiation

Fong Shu Yee

School of Health Sciences  
Universiti Sains Malaysia  
Health Campus  
16150 Kubang Keratan, Seremban  
Malaysia

## CERTIFICATE

This is to certify that the dissertation entitled

**Uniformity, sensitivity, linearity, and hot region image analysis by employing unconventional filter technique (Cu 0.125mm and Al 0.2mm) with Tc-99m in SPECT imaging**

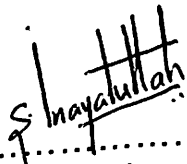
is the bonafide record of research work done by

**Ms. Fong Shu Yee**

during the period from **November 2003 to March 2004**

under my supervision.

Signature of Supervisor:



.....  
Dr. Sayed Inayatullah Shah  
School of Health Sciences  
Universiti Sains Malaysia  
16150 Kubang Kerian  
Kelantan, Malaysia

Date: 22/4/2004.....

## **ACKNOWLEDGEMENTS**

I would like to acknowledge my appreciation to everyone who has helped me tremendously in producing this dissertation.

Firstly, heartfelt thanks goes to my supervisor, Dr. Sayed Inayatullah Shah, for his continuous assistance and advice throughout the period of this study. I cannot thank him enough for his great patience, enthusiasm and effort in developing my knowledge, understanding and experience in the field of research and experimental management.

I would like to express my gratitude to Associate Professor Dr. Ahmad Zakaria, coordinator of Medical Radiation course, for his constant concern and encouragement during my experiments and thesis writing.

My special thanks goes to Mr. Khairul Nizam, technician of The Department of Radiotherapy and Oncology, Hospital Universiti Sains Malaysia, who has been very kind and willing to stay up until late hours to aid me in my experiments. My sincere gratitude also goes to Mr. Abdullah Waidi, staff of School of Health Sciences, Universiti Sains Malaysia, for his guidance in reconstructing and analysing the images acquired in the experiments using computer.

My experimental work would not have been possible without the use of the facilities provided by The Department of Nuclear Medicine, Hospital Universiti Sains Malaysia, Kubang Kerian, Kelantan. I wish to thank all the dedicated and helpful staff members for their great assistance during my experiment, as well as providing a pleasant and friendly working environment.

I would also like to convey my warmest appreciation to my friend, Chloe Ng Ching Choe, for lending me her digital camera in order to capture photographs for better presentation of this dissertation. Special thanks also goes to Rita Ting Ling,

Yong Kim Far and Liew Kar Wai for their support and valuable comments. I also owe merit to Prema Devi, my course mate as well as my project partner, for her excellent technical assistance and various contributions during the project.

Finally, I would be greatly derelict in my appreciation if I did not extend my gratitude to my family, who has given me a lot of moral support, love and assistance when I faced difficulties in the process of doing this informative dissertation.

# TABLE OF CONTENTS

	Page
<b>Title</b>	<b>i</b>
<b>Certificate</b>	<b>ii</b>
<b>Acknowledgements</b>	<b>iii-iv</b>
<b>Table of contents</b>	<b>v-vi</b>
<b>List of tables</b>	<b>vii</b>
<b>List of figures</b>	<b>viii-ix</b>
<b>Abstract</b>	<b>1</b>
<b>Introduction</b>	<b>2-7</b>
<b>Review of literature</b>	<b>8-10</b>
<b>Objective of the study</b>	<b>11</b>
<b>Materials and Methods</b>	<b>12-26</b>
Gamma Camera System	12
Collimators employed	12-14
Choice of radionuclide	14
Selection of Material Filters	14-15
Phantom	15-19
Preparation of phantom for use	20
Image acquisition and reconstruction	20-22
Image analysis	22-26
<b>Results</b>	<b>27-53</b>
Uniformity	27-31
Sensitivity	32

Linearity	33-39
Hot region analysis	40-53
<b>Discussion</b>	<b>54-61</b>
<b>Conclusion</b>	<b>62</b>
<b>References</b>	<b>63-67</b>
<b>Appendix</b>	

## LIST OF TABLES

	<b>Page</b>
Table 1: Standard deviation values of transaxial slice of uniform cylindrical phantom without and with material filter Cu 0.125mm and Al 0.2mm using the LEGP and LEHR collimator	31
Table 2: Sensitivity values of transaxial slice of uniform cylindrical phantom without and with material filter Cu 0.125mm and Al 0.2mm using the LEGP and LEHR collimator	32
Table 3: Profile curve of a horizontal area in the middle of the cross grid of the linearity insert in cylindrical phantom without and with material filter Cu 0.125mm and Al 0.2mm using LEGP and LEHR collimators	38
Table 4: FWHM values of horizontal area in the middle of the cross grid of the linearity insert in cylindrical phantom without and with material filter Cu 0.125mm and Al 0.2mm using LEGP and LEHR collimators	39

## LIST OF FIGURES

	<b>Page</b>
Figure 1: Imaging unit used in this study (GCA-901A/HG)	13
Figure 2: Construction of a material filter	15
Figure 3: An acrylic walled cylindrical phantom (Ray A. Carlson)	16
Figure 4: Exploded view of the phantom (Ray A. Carlson)	17
Figure 5: Schematic cross-sectional view of 'hot' regions insert	18
Figure 6: Schematic cross-sectional view of linearity insert	19
Figure 7: Rotation of detector to obtain sixty views	21
Figure 8: Selection of horizontal area in the middle of the cross grid of the linearity insert	24
Figure 9: Transverse image slices of a uniform section of cylindrical phantom (A) without material filter, (B) with Cu 0.125mm filter and (C) with Al 0.2mm filter using LEGP collimator	28
Figure 10: Transverse image slices of a uniform section of cylindrical phantom (A) without material filter, (B) with Cu 0.125mm filter and (C) with Al 0.2mm filter using LEHR collimator	30
Figure 11: Transverse image slice of linearity insert of cylindrical phantom (A) without material filter, (B) with Cu 0.125mm filter and (C) with Al 0.2mm filter using LEGP collimator	34
Figure 12: Transverse image slice of linearity insert of cylindrical phantom (A) without material filter, (B) with Cu 0.125mm filter and (C) with Al 0.2mm filter using LEHR collimator	36
Figure 13: Transverse image slice of a hot region insert of cylindrical phantom (A) without material filter, (B) with Cu 0.125mm filter and (C) with Al 0.2mm filter using LEGP collimator	42
Figure 14: Transverse image slice of a hot region insert of cylindrical phantom (A) without material filter, (B) with Cu 0.125mm filter and (C) with Al 0.2mm filter using	45

LEHR collimator

Figure 15:	Hot region contrast values of 30mm, 22.4mm and 17.9mm diameter without and with material filter using LEGP collimator	46
Figure 16:	Hot region signal-to-noise ratio values of 30mm, 22.4mm and 17.9mm diameter without and with material filter using LEGP collimator	47
Figure 17:	Hot region standard deviation values of 30mm, 22.4mm and 17.9mm diameter without and with material filter using LEGP collimator	48
Figure 18:	Hot region PRMSN values of 30mm, 22.4mm and 17.9mm diameter without and with material filter using LEGP collimator	49
Figure 19:	Hot region contrast values of 30mm, 22.4mm and 17.9mm diameter without and with material filter using LEHR collimator	50
Figure 20:	Hot region signal-to-noise ratio values of 30mm, 22.4mm and 17.9mm diameter without and with material filter using LEHR collimator	51
Figure 21:	Hot region standard deviation values of 30mm, 22.4mm and 17.9mm diameter without and with material filter using LEHR collimator	52
Figure 22:	Hot region PRMSN values of 30mm, 22.4mm and 17.9mm diameter without and with material filter using LEHR collimator	53

## **ABSTRACT**

In SPECT imaging, the presence of the scattered events in projection data affects the overall quality of the image as well as the quantification of the radioactivity distribution. In this study, material filter method has been employed in the attempt of reducing the influence of scatter events in the measured counts. Such a filter decreases the relative contribution of scattered gammas by preferentially removing them before they can reach the surface of the detector of the gamma camera. The material filters used are copper (Cu) sheet 0.125mm thick and aluminium (Al) sheet 0.2mm thick. Filters are separately mounted on the face of a gamma camera (GCA-901A/HG) with either low energy general purpose (LEGP) or low energy high resolution (LEHR) collimators.

SPECT images of the insert simulating 'hot' lesions in cold background, linearity and the uniform section of the Carlson phantom loaded with Tc-99m are obtained without and with material filter.

The performance of the tomographic system is explored via the uniformity, sensitivity and linearity measurements, as well as the image lesion (hot) contrast, signal-to-noise ratio, standard deviation and percent root mean square noise (PRMSN). From the results, material filtered data shows an improvement in all tested parameters at the cost of system sensitivity.

## INTRODUCTION

Nuclear medicine is a medical specialty, which is non-invasive and painless, that uses safe and cost-effective radionuclide techniques to diagnose and treat human diseases. Diagnostic procedures involve the detection of gamma photons emanating from inside the patient's body for the purpose of acquiring information about the distribution and uptake of certain substances within the body. A small amount of radionuclide in a suitable chemical form is administered to the patient and the distribution of activity in the body is determined by an external radiation detection system. Nuclear medicine is unique, as it does not seek merely to form an image of an organ of interest or the whole body but aims also to provide information on organ function.

Nuclear medicine diagnostic specialities can be categorized into Planar (Conventional) imaging and Tomographic imaging. Single view images of the object are taken in planar imaging. These images comprise two-dimensional representations of a three-dimensional distribution of radioactivity in the detector field of view. Meanwhile, in tomographic imaging, emission tomographic data are obtained by taking a number of views around the object. Modern emission tomography is divided into two main groups which are the Single Photon Emission Computed Tomography (SPECT) and the Positron Emission Tomography (PET). This research involves the evaluation of image quality using two material filters associated with SPECT, a technique in which transverse sectional views of the body are obtained.

The basic principle used by a SPECT system specifically using a rotating camera is that a series of planar images are collected while the camera is rotated around the axis of rotation through either 180° or 360° around the patient (Todd-

Pokropek A, 1993). These planar images are used to create images of transaxial slices by some tomographic reconstruction process, often filtered back-projection (Germano G, 2001). This concept of reconstruction of tomographic images from projection images were pioneered by Bracewell and Riddle in 1967 for astronomic applications and was extended to medical imaging by Shepp and Logan (1974).

The aim of SPECT is to provide images of the radionuclide distribution present in the object being scanned (Yanch JC *et al.*, 1988). In many clinical diagnostic situations, visual interpretation and semi-quantitative analysis of SPECT images is performed and the accuracy of diagnosis depends upon image quality. However, the image quality in SPECT is affected by the characteristic of the SPECT system, by some physical phenomena (scatter, attenuation, septal penetration, partial volume effect), by tomographic reconstruction and by physiological factors such as patient motion. In all these factors, the problem of scatter via the Compton process, has given rise to many investigations due to its blurring effect (Buvat I *et al.*, 1995).

In Compton scattering interacting  $\gamma$ -rays or x-rays lose some energy and change the original direction. The change in the direction of many  $\gamma$ -rays that originate outside the field of view of the collimator causes them to be scattered toward the radiation detector, thus conveying poor information regarding their emission position. Consequently, the inclusion of Compton scattered gamma photons in the image will reduce the spatial resolution in the image, decrease the image contrast and reduce the signal-to-noise ratio. This leads to an overall degradation in the perceived quality of the image and cause errors in the quantification of the radioactivity distribution.

Since the main objective of SPECT imaging is to obtain good quality images, it is thus essential to maintain the superior performance of the whole system. With development of the first radioisotope scanners, there has been a continuous interest in procedures which could be applied to adequately assess and characterize the physical parameters of the system involved (Craddock TD, 1968). In this regard, a number of users of radioisotope scanning devices have made attempts to arrive at an acceptable method (Mallard JR, 1965; Goodwin PN and Himmelstein E, 1977; Jaszczak R *et al.*, 1984; Mueller *et al.*, 1986; Shah SI *et al.*, 2000).

One of the basic and important approaches towards the characterization of the scanning system is the uniformity. Basically, uniformity is just the non-stationarity of the sensitivity response of the detecting system that is the number of observed counts at given position when the input activity distribution was known to be uniform. In other words, uniformity is conventionally defined as the ratio between the mean response to a uniform object and the response at a given position. This parameter has a certain distribution, which is not normally regular in either space, or with respect to other parameters (such as energy), although it does change as a result of statistical fluctuation as a function of the number of events detected (Gullberg GT, 1987). This parameter is essential to check that the response of the detector to a uniform irradiation is uniform within defined limits. Field non-uniformity artifacts have a "bull's eye" appearance with alternating concentric rings of high and low intensity due to regional sensitivity variations in the projection images (Mark WG and William DE, 2001). A simple method for assessing tomographic uniformity is to scan a reasonably large cylinder of circular or elliptical cross section and slice obtained after

reconstruction is examined for uniformity artifacts through visual inspection and the standard deviation in the image average count density. However, no generally accepted method for existing tomographic uniformity exists yet and it is still the subject of ongoing research (Todd-Pokropek A, 1993).

Another parameter for a SPECT system is sensitivity. The sensitivity of a SPECT imaging device is a measure of its ability to detect  $\gamma$ -rays photons efficiently (Ramesh Chandra, 1992). The sensitivity depends upon the total solid angle subtended by the detector at the source. There are several techniques of measuring the sensitivity of an imaging system, such as by scanning point sources, flood sources or cylindrical phantoms. Scanning a cylindrical phantom filled with low radioactivity concentration is a commonly used method. In this case, the effect of system dead time may be eliminated. Sensitivity can be measured from a single slice and total phantom volume, and expressed as cps/(mCi/ml) or cps/(MBq/ml). Poor sensitivity can only produce noisy and low-resolution images. This is especially true since tomographic reconstruction dramatically amplifies the stochastic noise inherent in radioactive decay (Shah SI *et al.*, 2000).

Linearity is also a fundamental requirement for a SPECT system. This parameter deals with the ability to reproduce a linear activity source as linear in the image. A phantom with a linear arrangement of bars or holes is usually used. The image produced should look exactly like the phantom, that is straight lines should be reproduced as straight (Donald RB *et al.*, 1997). Linearity expresses the relationship between observed numbers of photon, and emitted numbers of photon (Todd-Pokropek A, 1993). Normally, count loss because of dead time

effects is not a problem in SPECT. Conversely, changes in linearity as a result of scatter and attenuation are very significant.

In medical imaging, emphasis is placed on the detection of abnormalities, by differentiating lesions from the background and by examining the shape and position of a lesion. This task is made more difficult when the contrast is lower between the lesion and the background. Beside the parameter of SPECT system performance, quality of image is also assessed by measuring the lesion contrast signal-to-noise ratio and standard deviation (Shah SI, 1996). Moreover, quality of images can be inspected visually and practical qualitative results can be obtained due to the excellent pattern recognition abilities of human perception. Nevertheless, small differences are more difficult to assess quantitatively and hence errors can occur.

Image lesion contrast is usually expressed as the regional change in photon density in a target area to that in the surrounding field or in an adjacent area. In addition, the concept of contrast is a generalized form of modulation. While modulation applies to cyclic distribution, contrast can be applied to any type of distribution and the contrast of one region in a distribution with respect to another can be calculated based on standard formula.

It is essential to evaluate the signal-to-noise ratio for various imaging conditions. It is because the amplification of noise by the reconstruction filter decreases the expected signal-to-noise by factors of ten or more (Budinger *et al.*, 1979). In order to obtain the image lesion signal-to-noise ratio, a standard formula is employed (Gilardi *et al.*, 1988).

Radiation events such as count values are distributed in a very special way. The value of standard deviation, expressed in number of counts, is related

to the actual number of photons detected during image acquisition. Theoretically, the value of standard deviation is the square root of the average of the squares of the deviation of the value of a set of measurements from each of the individual measurements. In actual practice, the true count value is never known. In most cases, measurements value will be sufficiently close to the true value (Perry Sprawls, 1995). Thus, standard deviation allows the quantitation of the concepts of precision and accuracy emerges frequently in statistical analysis of SPECT images.

In the light of the above facts, the present study was undertaken to investigate the feasibility of utilizing material filters such as copper and aluminium sheet mounted separately in front of the collimator, in order to obtain good qualitative and quantitative images.

## REVIEW OF LITERATURE

The literature review reveals that some work has been done on improving the image quality and performance of scintillation cameras using unconventional (material) filter techniques.

The use of filters to improve the performance of scintillation cameras was proposed some time ago by Muehllehner *et al.*, (1974). The filters were placed over the detector face, tailored for Tc-99m (140keV) and consisted of 0.23 mm of tin, as the primary absorber and 0.13 mm of copper. The aim was to attenuate preferentially the lower energy events in the  $\gamma$ -ray spectrum while leaving the photopeak events relatively unchanged. The dead time associated with the low energy events could thus be reduced. In their study, improvement in count rate performance was achieved only at high count rates but reduced slightly at low rates.

The effect of filters was subsequently studied again by Muehllehner (1975) for a positron imaging system consisting of two scintillation cameras. The filters in this case comprised of 1.27 mm of lead, 0.76 mm of tin and 0.25 mm of copper. In contrast to earlier work where only the photopeak was used, it was shown that Compton events in the crystal (followed by escape of the secondary  $\gamma$ -rays) could be used to form an image if the  $\gamma$ -rays scattered in the object were largely eliminated by the filters. A factor of five increases in useful count rate was reported.

In 1975, Harshaw Scintillation Phosphors indicated that there is possibility to design an appropriate absorbing filter by combining various detector materials. Shortly after this report, Strand and Larsson (1978) published a paper in which

they suggested that it may be possible to reduce the recording of scattered photons by means of specially made attenuating filters.

Later in 1986, Pillay and his colleagues applied an alloy (composite) filter, consisting of Pb, Zn and Sn, in single photon emission (Planar) imaging. They reported improvement in the quality of images from various patient studies. In addition, they also mentioned in their paper that it could be possible to use the technique in SPECT as well.

Ficke and Ter-Pogossian (1990), suggested that material filters might be advantageous in reducing low energy radiation originating in the field of view of the scanner. They analysed the spectrum from NaI(Tl) detectors by employing 0.43 mm and 0.86 mm thick lead (Pb) filters in PET. As a result, low energy events were reduced by some 30-40% for the loss of 7-12% photopeak (unscattered) events.

A few years later, Pollard *et al.*, (1992) used lead sheets for imaging therapeutic doses of I-131 labelled with monoclonal antibody. In their study, they attached 1.6-6.4 mm thick Pb sheets to the front face of the gamma camera. They also applied Monte Carlo study by simulating a gamma camera and a sheet of lead material mounting on it. Consequently, they found that the system resolution is degraded with lead sheet. Nevertheless, they could not apply the technique in SPECT imaging because of absorber's weight. Although they suggested the use of such absorbers in single photon emission tomography to reduce the detection of unwanted photons from the data, the application was limited only to the situation where the camera system is able to accurately rotate the additional weight.

In the light of the above ideas, Spinks TJ and Shah SI (1993) undertaken a study to investigate the effects of lead (Pb) filters (0.5 mm and 0.1 mm thick ) on the overall performance of a multi-ring positron tomography designed for brain imaging in which data is routinely acquired in 3D mode with septa retracted. In their study a significant reduction in low energy events (50 - 200 keV) was obtained as well as a decrease in random rates and percent dead time.

In 1995, Shah SI employed the unconventional filter technique in reducing the influence of scatter gammas on SPECT data. The ultimate objective was to enhance image quality and to achieve accurate quantitative measurements of the radioactivity distribution in SPECT images in clinical applications. In his study, 0.25 mm thick tin (Sn) material filter was used and it was shown clearly that not only image quality but also quantification of counts can be improved by the use of novel scatter and attenuation correction procedures using material filter.

More recently, Shah SI and Sidney Leeman (2002) reported the effects on spatial resolution and MTF using Sn material filter in conjunction with a standard energy window was measured. Results obtained from the data that were acquired with material filter show an overall improvement. It was concluded that the technique could be useful for some SPECT clinical studies.

## **OBJECTIVE OF THE STUDY**

The objectives of this study are:

1. To obtain images without and with unconventional filter technique (Cu 0.125mm and Al 0.2mm) by scanning phantom with Tc-99m in SPECT imaging.
2. To study the gamma camera performance parameters, via; uniformity, sensitivity and linearity with Tc-99m without and with unconventional filter in SPECT imaging.
3. To study hot region image quality with Tc-99m without and with unconventional filter in SPECT imaging with respect to the contrast, standard deviation, signal-to-noise ratio and percent root mean square noise of the image.
4. To compare the improvement in gamma camera performance parameters and image quality in Tc-99m SPECT imaging using unconventional filter with those obtained without material filter data.

## **MATERIALS AND METHODS**

### **Gamma Camera System**

The most important equipment used in this study is the multi-purpose GCA-901A/HG digital gamma camera system, manufactured by Toshiba Medical System. It incorporates a rotating gamma camera (Model number NDDT901B) and operator console (Model number NCOC001A). The general specifications of the detector, as well as the operator console are given in Appendix in Tables i and ii respectively.

The revolving gantry on which the camera is mounted consists of a large stationary steel support stand, midway between the camera and a counter weight. The camera supporting arms are attached to the support stand, in such a way that the camera may be rotated at any desired radius (Figure 1).

### **Collimators employed**

For SPECT imaging, low energy general purpose (LEGP) and low energy high resolution (LEHR) collimators are used and mounted on the face of the detector of the gamma camera. A collimator allows only those gamma-photons traveling along certain specified directions to reach surface of the crystal of a scanning system. The precise collimation of the gamma-photons is essential not only to obtain accurate spatial distribution of the gamma-photon emitting radionuclides, but also to eliminate at least some of the scattered gammas which would impair contrast.

For optimal performance of SPECT with a scintillation camera, choice of a collimator is very important. In this study, two low energy parallel-hole collimators

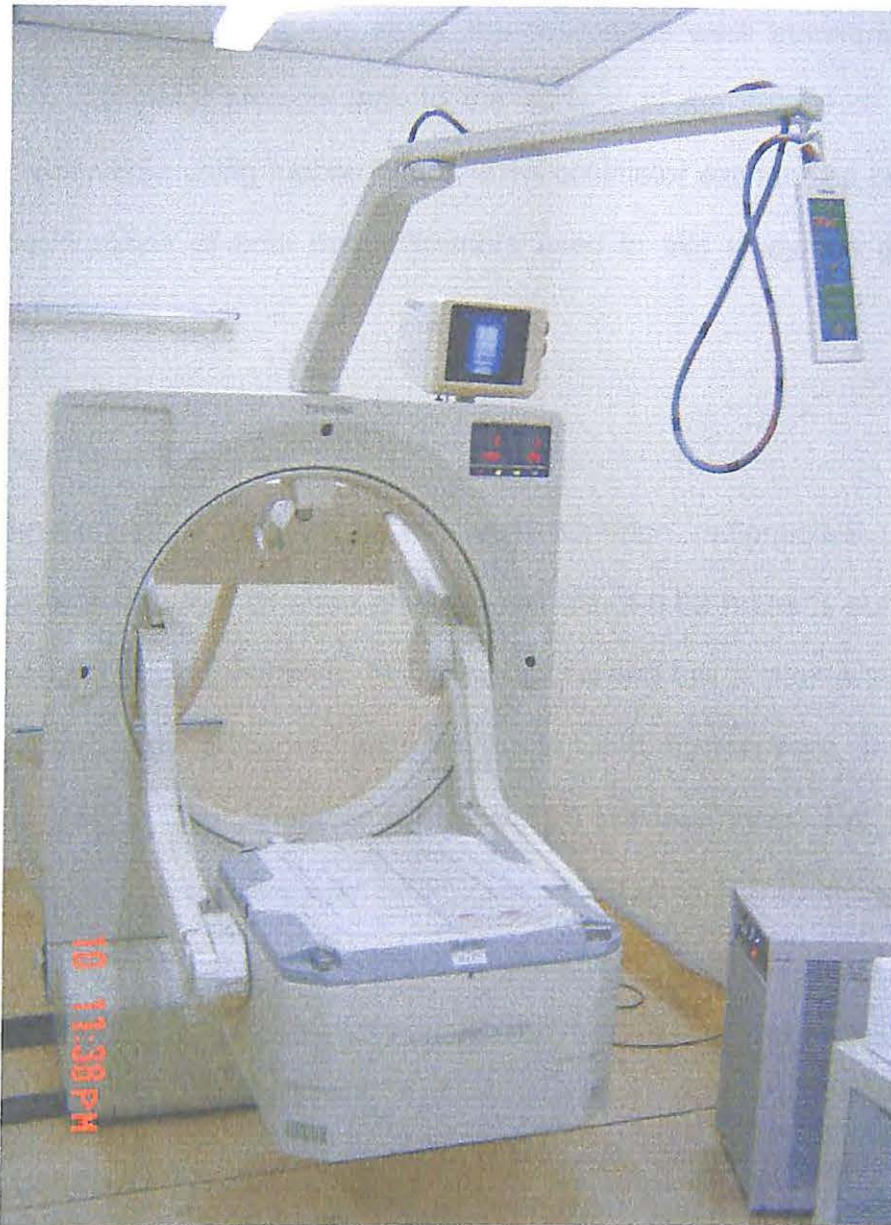


Figure 1: Imaging unit used in this study (GCA-901A/HG)

were employed, namely LEGP and LEHR. Both of the collimators are manufactured by Toshiba Medical System. The reason for this choice was that these collimators are the most heavily used for clinical studies in nuclear medicine departments. During this study, the collimators were transferred from the RDV-91A collimator storage rack to the surface of the crystal of gamma camera, or vice versa using mobile NGEC 901A collimator exchanging cart. The general specifications of both the collimators used in this study are given in Appendix in Tables iii.

### **Choice of radionuclide**

Technetium-99m (Tc-99m) is the most common radionuclide used in nuclear medicine imaging. Its short physical half life of 6.02 hours is sufficiently long for many applications. It emits 140 keV photons and this photon energy has satisfactory tissue penetration and yet readily collimated. Furthermore, its photon energy also gives a high detection efficiency with the thin crystal NaI(Tl) of a gamma camera (100% efficiency for 140keV, with crystals of 1.27cm thickness or greater). Tc-99m was the radionuclide of choice in this study because of its properties mentioned above and also its availability and cost effectiveness.

### **Selection of Material Filters**

As the aim of this study is to obtain image without and with filter mounted on the outer surface of the collimator, two different materials were chosen as the filter. Copper (Cu) 0.125mm thickness and aluminium (Al) 0.2mm thickness were prepared and both are cut into a rectangular size of 46cm X 56.5cm. A

rectangular shaped frame of aluminium (Al) strips was made, on which the filter is fitted, as depicted in Figure 2.

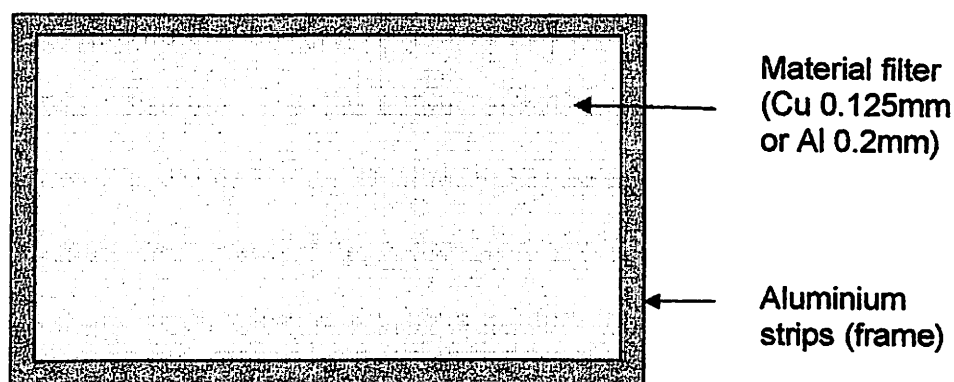


Figure 2: Construction of a material filter

### Phantom

An acrylic walled cylindrical phantom (Ray A. Carlson) was used in this project, as illustrated in Figure 3. It consists of a tank and an assortment of inserts, which includes the 'cold', 'hot' lesion and linearity inserts (Figure 4). The dimensions of the tank are 21.25cm outer diameter, 20cm inner diameter and 31.25 cm in length acrylic cylinder, which has an 'O'-ring sealed covered with fill and drain ports.

The 'cold' lesion insert is a 7.5cm thick and 20cm outer diameter acrylic block employed to simulate 'cold' regions in a hot background. It contains 7 plastic rods whose diameters are 5.9mm, 7.3mm, 9.2mm, 11.4mm, 14.3mm, 17.9mm and 22.4mm and each rod is 25% larger in diameter than the preceding one. Plastic spheres of the same diameter as the rods can be attached on stand-off supports to the outside of this insert.

Meanwhile, the 'hot' lesion insert is a 6.35cm thick and 20.00cm outer diameter acrylic block used to simulate 'hot' lesions in a cold background. Eight

pairs of circular holes (in a 'V' shape) are drilled through the block, each pair separated by a distance equal to the hole diameters (4.7mm, 5.0mm, 7.3mm, 9.2mm, 11.4mm, 14.3mm, 17.9mm and 22.4mm). The distance of each pair is 25% larger than the preceding pair. In addition, the insert consists of two pairs of holes of 30mm diameter near the edges (opposite to each other at 180° from the centre of insert) to the insert, as depicted in Figure 5.

The linearity insert is a 5cm thick and 20cm outer diameter acrylic block with crossed grid of channels cut out in a 3.75cm deep square pattern, as shown in Figure 6. In this study, only the images from the 'hot' lesion, linearity insert and uniform region are included.



Figure 3: An acrylic walled cylindrical phantom (Ray A. Carlson)

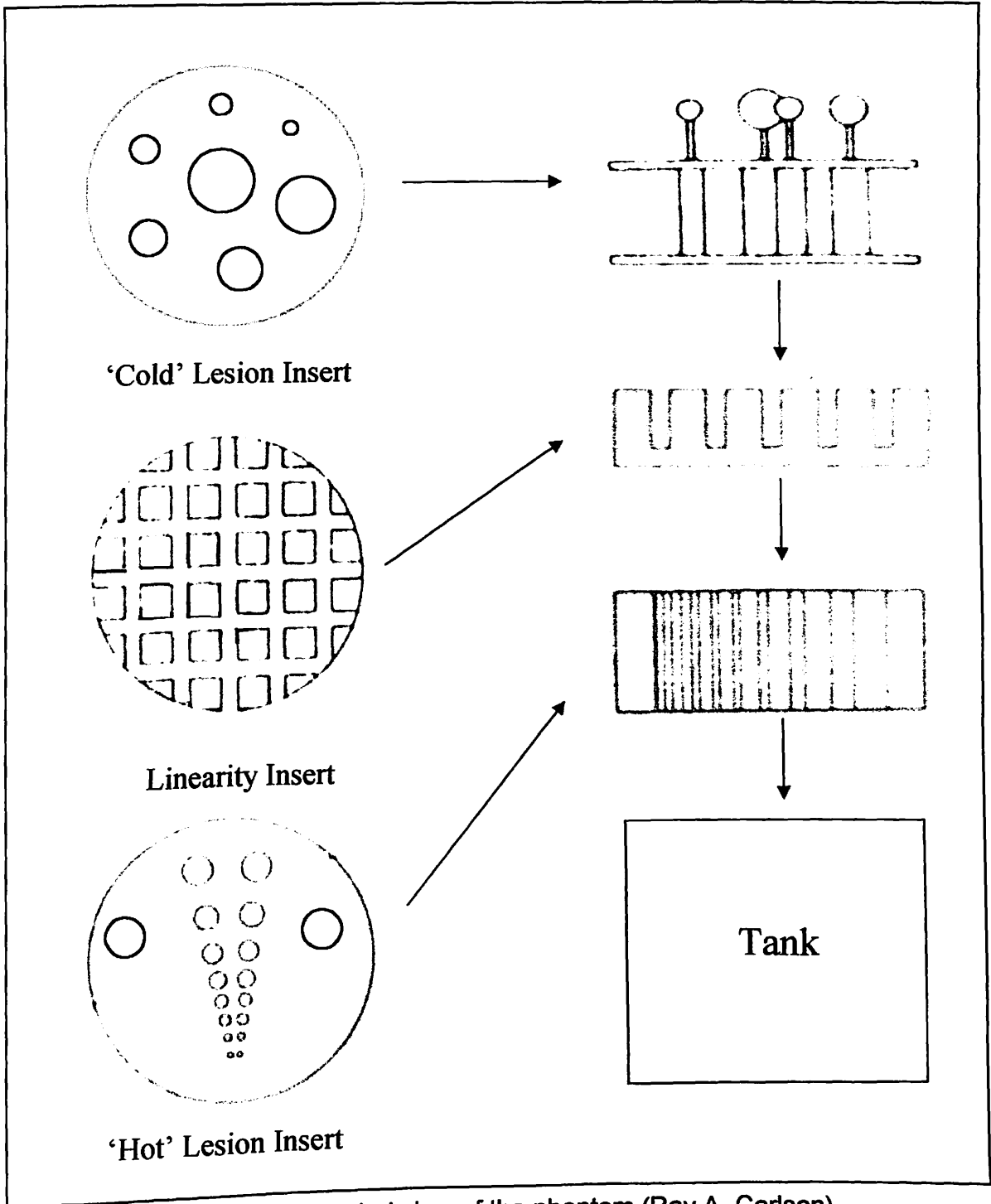


Figure 4: Exploded view of the phantom (Ray A. Carlson)

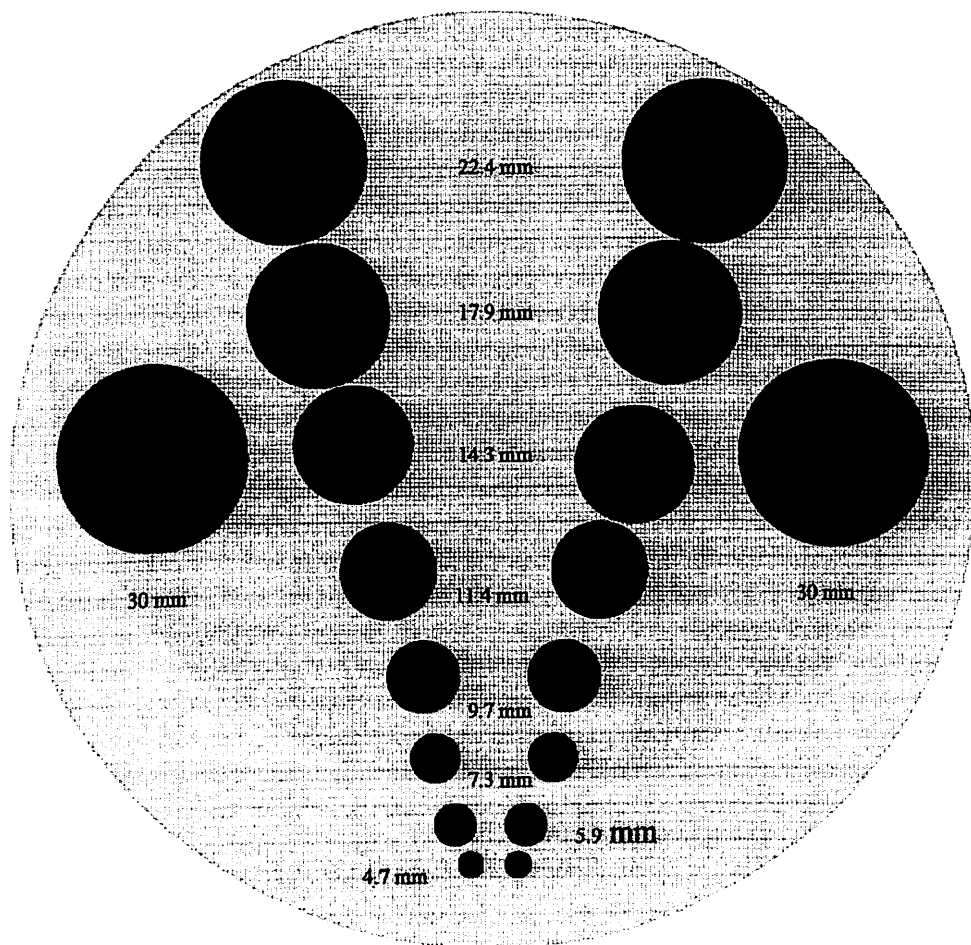


Figure 5: Schematic cross-sectional view of 'hot' regions insert

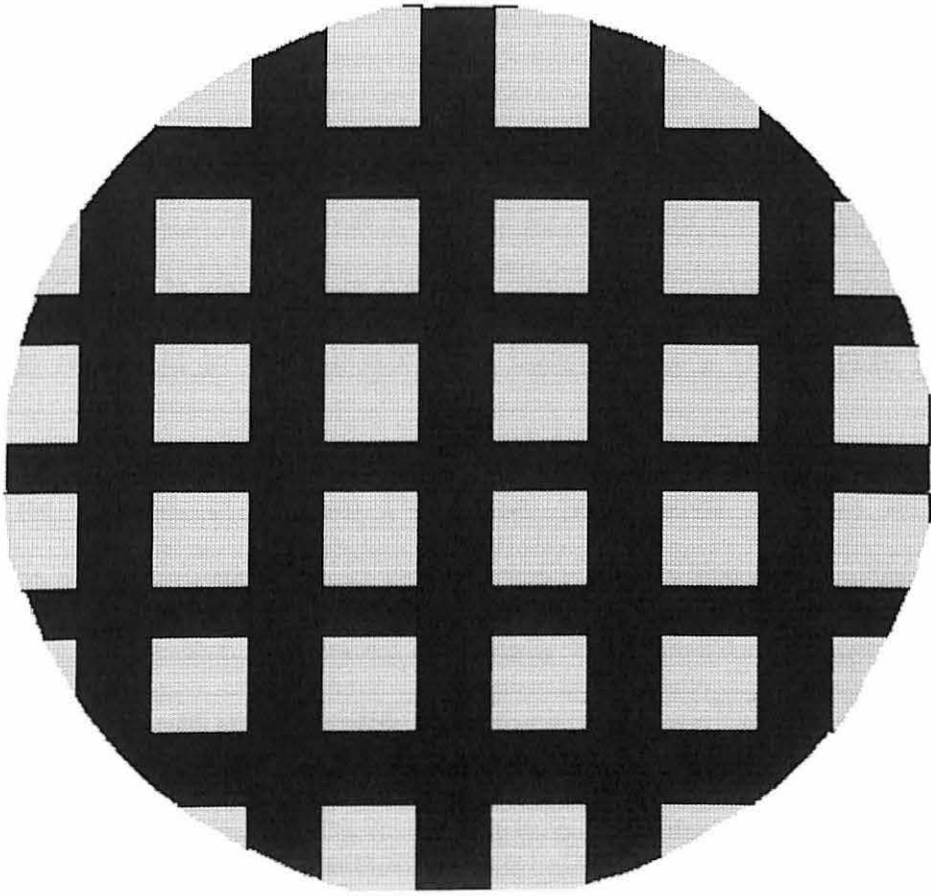


Figure 6: Schematic cross-sectional view of linearity insert

This study was conducted using the scanning unit described in section gamma camera system on page 12. The data were acquired by placing material filters (either 0.125mm thick copper sheet or 0.2mm thick aluminium sheet) on the face of collimators with LEGP or LEHR collimators as well as without any filter by scanning a Tc-99m filled acrylic cylindrical phantom.

### **Preparation of phantom for use**

The Carlson phantom was prepared by filling the water into the tank and the hot and linearity inserts were placed in the phantom tank. The phantom was put aside overnight to allow dissolve air bubbles if any to dissipate from the water.

The solution of Tc-99m (19.29mCi) was added into the tank. This procedure was done carefully to avoid any spillage of the radioactive solution. The solution in the tank was mixed thoroughly by repeated inversion of the tank until the phantom was ready for use.

### **Image acquisition and reconstruction**

The phantom filled uniformly with Tc-99m solution was placed on the patient couch, with axis parallel to the face of the collimator and in the centre of the field of view (FOV) of the gamma camera. The phantom was taped securely in position on the patient couch to prevent movement which might affect the image quality. The image was acquired by using LEGP collimator which was mounted on the face of the detector of the gamma camera without using any material filter. The data were acquired within a symmetrical energy window of 126 keV to 154 keV (centred at 140 keV) and 128 x 128 imaging matrix. Sixty views

were taken over 360° and the time for each projection/view was 20 seconds (Figure 7). The radius of rotation of the gamma camera was 20 cm from the central axis of the phantom.

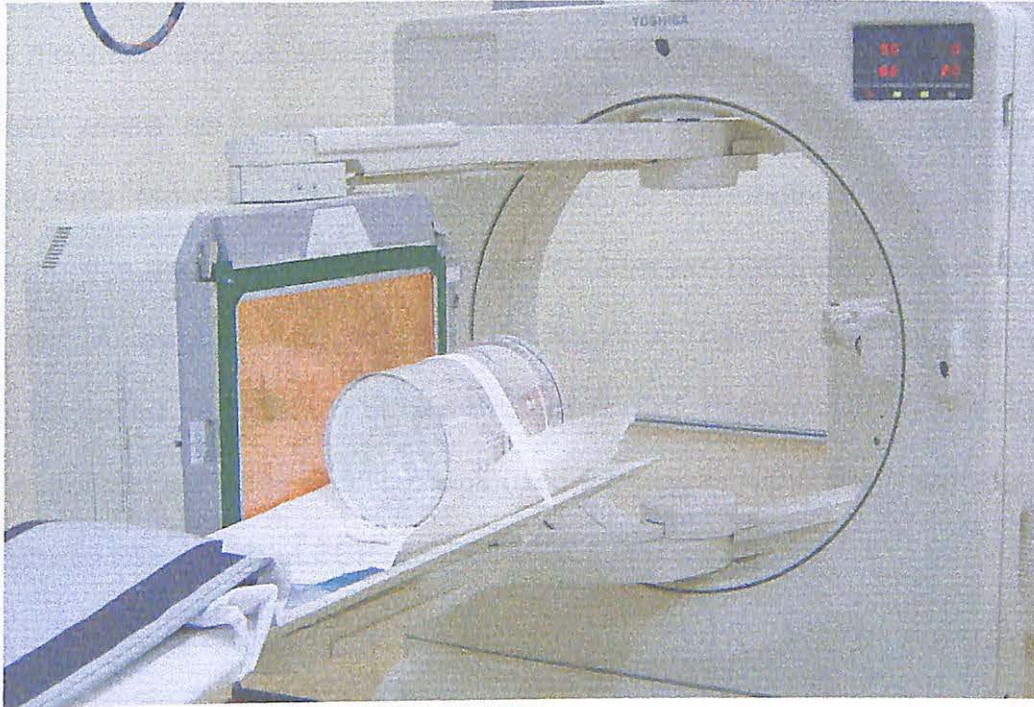


Figure 7: Rotation of detector to obtain sixty views

After that, the acquisition of images was repeated by mounting a filter Cu 0.125mm thick on the outer surface of the collimator. The acquisition parameters were the same as those without material filter. The study was continued by using 0.2mm thickness of aluminium (Al) as the material filter.

The whole procedure of image acquisition without and with material filter of Cu and Al was repeated by using the LEHR collimator. The position of gamma camera and phantom throughout the study remained unchanged.

Transaxial images of the 'hot' region insert and linearity insert, as well as uniform section of phantom were reconstructed by the filtered back projection method. A ramp filter with a 8<sup>th</sup> order Butterworth window having 0.15 cycles/cm

cut-off frequency was used for the data collected within the photopeak energy window. For the attenuation correction technique, postreconstruction (Chang's method, 1978) was selected. The attenuation coefficient value of 0.141/cm for Tc-99m was applied to the photopeak data in the case where the material filter was mounted, and an effective attenuation coefficient value of 0.131/cm was chosen where no material filter was employed. This choice of attenuation coefficients represents a more severe test of the material filter, since it presupposes that some scattered gamma photons are preferentially removed by the filter. All data were corrected for the decay of Tc-99m. The raw data were also corrected for the uniformity and center of rotation (COR). The same reconstruction algorithm and filter was used for images without and with Cu and Al material filter for both LEGP and LEHR collimators.

### **Image analysis**

For uniformity and sensitivity analysis, the 7<sup>th</sup> slice was selected among those were reconstructed from the uniform region of the phantom. A large circular region of interest (ROI) comprising 1451 pixels, was drawn on the image and from which were derived the system uniformity, sensitivity and standard deviation. The same ROI was used for both without and with material filter images. Visual inspection of the reconstructed images was performed to compare the uniformity of images obtained without and with material filter. Values of standard deviation in the average count density of the ROI selected on the slice of images without and with material filter were tabulated and compared to determine the uniformity among all the images.

Using the same single slice, the sensitivity was measured based on the equation 1 and expressed as cps/(mCi/ml).

$$\text{Sensitivity} = \frac{N}{V} \quad (1)$$

Where N is the total number of events registered during an effective time and V is the unit of activity concentration in a phantom of given size.

The study was continued by selecting the 32<sup>nd</sup> slice for the linearity analysis of the linearity insert. Visual inspection was carried out to assess the linearity of the slice by detecting any distortion of the shape of the lines. In addition, the horizontal area in the middle of the cross grid of the linearity insert was chosen by drawing the lines, as shown in Figure 8. The same area was used for both without and with material filter images. The line profile of the selected area was obtained through the computer system using the image analysis package (GMS-5500). The full-width at half-maximum (FWHM) value of the horizontal area in the middle of the cross grid of the linearity insert was also obtained.

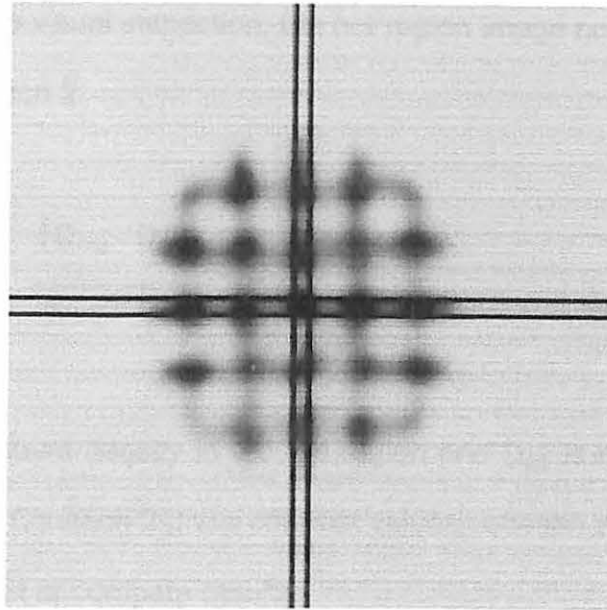


Figure 8: Selection of horizontal area in the middle of the cross grid of the linearity insert

In the hot region analysis, the 44<sup>th</sup> slice was selected. ROI was drawn on the selected hot regions of the image. In this analysis, only three pairs of hot regions of the same diameter each pair (opposite to each other at 180°), were considered because other pairs of hot regions were not clear and it was difficult to set the ROI inside them. The hot regions diameters are 17.9 mm, 22.4 mm and 30 mm. The same ROI was employed for both without and with material filter images using LEGP and LEHR collimator. For hot regions, image quality is assessed qualitatively, by visual inspection and quantitatively, by evaluating image lesion contrast, signal-to-noise ratio, standard deviation in the count density of hot region ROI and percent root mean square noise (PRMSN). Average values of the each pair of hot regions of same diameter and symmetrically placed in the phantom were employed to obtain the image contrast, signal-to-noise ratio, standard deviation and PRMSN.